

A CNN-LSTM Deep Learning Classifier for Motor Imagery EEG Detection Using a Low-invasive and Low-Cost BCI Headband

Francisco M. Garcia-Moreno
Dept. of Software Engineering
University of Granada
Granada, Spain
0000-0001-6366-3758

Maria Bermudez-Edo
Dept. of Software Engineering
University of Granada
Granada, Spain
0000-0002-2028-4755

María José Rodríguez-Fortiz
Dept. of Software Engineering
University of Granada
Granada, Spain
0000-0002-3166-6652

José Luis Garrido
Dept. of Software Engineering
University of Granada
Granada, Spain
0000-0001-7004-1957

Abstract—Brain Computer Interfaces (BCI) can be used not only to monitor users, recognizing their mental state and the activities they perform, but also to make decisions or control their environment. Hence, BCI could improve the health and the independence of users, for example those with low mobility disabilities. In this work, we use a low-cost and low-invasive BCI headband to detect Electroencephalography (EEG) motor imagery. In particular, we propose a deep learning classifier based on Convolutional Neural Networks (CNN) and Long Short-Term Memory (LSTM) in order to detect EEG motor imagery for left and right hands. Our results report a 96.5% validation accuracy in the correct classification. Additionally, we discuss the influence of using raw data over using the data split in frequency bands in the model proposed. We also discuss the influence of certain frequency bands activity over other frequency bands in the task proposed. These results represent a promising discovery in order to democratize users' independence by the adoption of low-cost and low-invasive technologies in combination with deep learning.

Keywords—Neural networks, deep learning, EEG signals, motor imagery, BCI, user's interaction

I. INTRODUCTION

Health care professionals are beginning to use wearable devices for patient monitoring and clinical practice, which can be combined with machine learning algorithms to analyze the collected data and consequently predict, prevent or design an intervention plan [1]. Wearables with different kinds of built-in sensors (mechanical, physiological, bioimpedance and biochemical) can measure the physical and mental state of the individuals. They can also act in wider domains as input or output devices to allow users to interact with the environment. For example, some wearable devices such as smart glasses and vibration bracelets (sometimes in combination with other static sensors in the environment, e.g. camera, presence, etc.) provide feedback about users' interactions or guidelines in performance during activities of daily living (ADLs) such as cooking, shopping, etc. Some commercial wearables could replace or be equivalent to expensive medical devices in particular cases. This kind of devices leads to new possibilities in research; their main benefits are that they can be used outside, anytime and anywhere, not only in clinical environments. They can gather

big quantities of data in an objective and precise way. One of the areas of healthcare in which wearables are applied is the evaluation and intervention in healthy ageing. There are a lot of research projects on evaluation or intervention systems that use wearable devices, for example, to help the elderly living independently, increasing their autonomy and improving their life quality [2], [3].

In our previous work [4], we explored the wearable capabilities collecting data by proposing an solution-oriented system/software architecture that provides suitable support for machine learning models in order to predict the frailty status of older adults. In this paper, the aim in the healthy aging domain is to explore the potential of the commercial Brain Computer Interfaces (BCI) devices, specifically the wearable and low-cost Muse headband, made by InteraXon [5]. The built-in Muse headband sensors record Electroencephalography (EEG) signals through four channels located around the head of a person. These positions follow the 10/20 international system standards [6]. Regular BCI devices, used at hospitals, have up to 256 channels, which need to be in direct contact to the head skin at different locations and which involves expensive machinery and cables paired to the head of the user. None of the projects found and reviewed in healthy aging uses headbands despite their potential. The low-cost and low-intrusive headbands could replace regular EEG machinery for some tasks, especially in combination with machine learning techniques, which could learn different states of the mind.

Headbands can collect some EEG signals of the brain activity of the users that can be used to evaluate their mind state, to make decisions or to control their environment. Furthermore, different analyses of data from headbands can discover patterns or anomalies of the user's behavior. Even in the absence of movement, the headband can measure thinking activity, such as motor imagery or goal-oriented thinking, which can be used to interact with a computer system. For example, if the user is thinking on pressing a bottom of a PC scream, the headband could detect such thinking and an app analyzing the headband signals could eventually press the bottom.

In this paper we explore, as a first approximation, the possibilities that the Muse headband offers. Specifically, we

propose a deep learning model to detect left and right hands motor imagery using Muse headband. The potential of this research is that once we classify left and right hands motor imagery, we could combine this information with other sensors to inform about users' activities and health status, and even to recommend interventions to improve the independent life.

The rest of the paper is organized as follows. Section 2 reviews the state of the art concerning BCI devices and machine learning algorithms applied to motor imagery. Section 3 introduces the used material and methods, and also presents the deep learning proposal for classifying two motor imagery tasks: left- and right-hand movement imagery. The results of our experiments can be found in Section 4. And the last section summarizes the conclusions and future work.

II. BACKGROUND

In recent years deep learning is gaining momentum. An enormous amount of papers using deep learning have been published in different areas [7]–[10]. Health is one of such fields [10] and even deep learning is commonly used to analyse EEG signals [11]. However, most of the research uses high accurate and expensive devices, which are quite intrusive, as the users need to stick sensors all over his/her head, connected with cables to expensive machines [11]. Only a few researchers have experimented with low-price, and low-intrusive EEG devices, such as headbands [11]. For example, Bird et al. [12] have used Long Short-Term Memory (LSTM), that is a type of Recurrent Neural Network (RNN), to learn the attentional emotion and sentiment of one user while providing visual stimuli.

Muse headband has been used to test the precision in identifying users and a range of similar activities (listening to music, reading, playing computer games, relaxing and watching movies) in the experiment of Wiechert et al. [13]. Four people performed each of these activities ten times while wearing the headband, registering the five waves (alpha, beta, theta, delta and gamma) of each one of the four locations every 0,1 seconds. The dataset with the streams of data was analysed exploring four different classifiers: Decision tree, Random Forest, Support Vector Machines and Neural Networks. The three last classifiers reach better accuracy to predict persons (95%-100%), but the first classifier did not perform well (only 65% of accuracy). Regarding the prediction of activities, the classifiers were less accurate, being SVM the best classifier with a 75% accuracy.

For motion intentions, there are also some research works that use headbands. For example, a headband with 16 sensors, EMOTIV, was tested in 26 children [14]. The aim of this work was to explore two strategies to control the movement of objects (a real remote-control car and a computer cursor). The first strategy is the motor imagery, thinking about what hand should be moved to do the task of moving the object. The second one is the goal-oriented strategy, imaging the desired effect, which reach better performance. The data obtained in the experiment was analyzed with Cohen's kappa. The results show worst performance in children than on other relevant adult studies, which normally reach around 70% accuracy.

There are also some research works on motion intention that apply machine learning techniques and EEG signals. For example, Chen et al. [15], use LSTM to learn human intentions

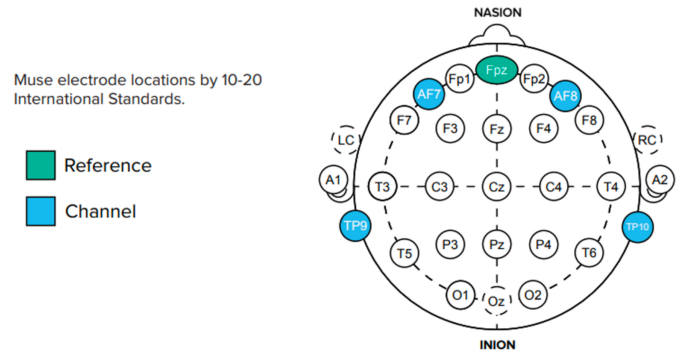


Fig. 1. Muse electrodes position [5]

to move hands, feet and eyes. However, they used high-cost and intrusive EEG devices. A few works have attempted to use headbands to learn the motion intentions of the users. For example, Rodriguez et al. [16] have applied Convolutional Neural Networks (CNN) and LSTM layers to learn the motion intention (hand and foot, relaxation state and mathematical activity) of one user with an accuracy of 80%. Another work [17], used Support Vector Machines (SVM), a traditional machine learning algorithm, for predicting left and right hands motor imagery getting an accuracy of 95,1%. This study included only one user and hence, they need to train the model for every new user. Furthermore, during long periods of times, between 3 and 7 seconds of signal recording, the accuracy was close to 95,1%, which could produce a model overfitting.

Our proposal improves the accuracy of these results ([16], [17]) in a similar experiment, discriminating between left and right hands motor imagery. We also increase the sample size over the previous works and control the overfit of the model.

III. METHODS

This section describes how to acquire EEG signals, to process them and to create a deep learning model for classifying two imagery motions: left- and right-hands movement intentions.

A. EEG signals acquisition

We used Muse headband version 2 by InteraXon [5], a wearable device with 4 electrodes (channels) to detect brain signals in a low-invasive way. Muse records EEG using 4 gold-plated cup bipolar electrodes, located on the sensorimotor brain cortex area. The location of the electrodes follows the 10/20 international standard presented in Fig. 1. These dry electrodes (or channels) are TP9 (left ear), AF7 (left forehead), AF8 (right forehead), TP10 (right ear) and Fpz, which is just the reference electrode, but it is not used to capture brain signals. Additionally, we used Mind Monitor [18], which is a mobile application (app), for recording the signals in real time. We did not use InteraXon software, because they discontinued its Software Development Kits (SDK), preventing software developers or researchers to create their custom Apps.

In the headband, each channel captures a raw EEG signal, measured in microvolts (μ V). Thus, in total we have four raw EEG signal data. These raw data are ranging from 0 to 1682μ V approximately. In addition, the Mind Monitor app supports



Fig. 2. A user during a recording session

collecting the values of the five brain wave types. Mind Monitor processes automatically the raw data to obtain the brain waves at different frequency bands, using the logarithm of the Power Spectral Density (PSD) of the raw EEG data coming from each channel. Therefore, five brain frequency ranges are recorded. In ascending order this frequency bands are: (1) delta ($< 4\text{Hz}$, appears for continuous-attention tasks), (2) theta (between 4 and 7 Hz, spikes when repressing a response or action), (3) alpha (between 8 and 15 Hz, measures relax or closing eyes), (4) beta (between 16 and 31 Hz, reflects active thinking, focus, high alert or anxiety), and (5) gamma ($> 32\text{Hz}$, displays during cross-modal sensory processing). Besides the EEG signals, Muse also has accelerometer, heart rate, breath and muscle movement sensors, allowing to record blinking and jaw clenching. Some of these sensors are neither supported for developers nor by the Mind-monitor app.

B. Trial protocol

We performed different EEG recording sessions with 4 healthy users aging from 33-55 (3 females; 1 male). We carry out recordings for detecting two different tasks: motor imagery for left and right hands with the eyeballs rotated in the respective direction, imaging to pick up a bottle, but avoiding to touch it, or to move the hand, or to blink eyes (See Fig. 2). According to Li et al. [17] the movement of eyeballs has influence on brain waves recorded by F7 and F8 electrodes (in our case AF7 and AF8, because these are the closest signals available in Muse).

Each recording takes 20 seconds of duration and they were repeated 20 times for each task. Thus, we labelled these recordings depending on the tasks: 0 for motor imagery for left hand; and, 1 for the right hand. These sessions took place in a silent and distraction-free environment.

C. Deep Learning

Deep Learning (DL), have been traditionally used for computer vision, speech recognition or natural language processing, and have been extended recently to several fields (LeCun et al., 2015). Also, in EEG signals deep learning have been successfully used in the last years [11].

DL, applies multiple iterative non-linear transformations of data, simulating the connections of the neurons in a brain. The parameters of the transformations are refined iteratively by

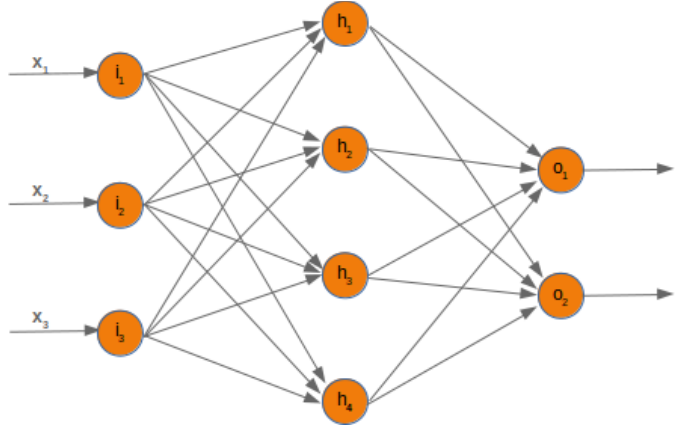


Fig. 3. Neural network with only one hidden layer [19]

minimizing a cost function (i.e. minimizing the error between the predicted and the real signal). DL means several layers of neural networks. However, there is not a consensus on how many layers make it deep. In practice, several deep learning approaches use just three layers. In a neural network we have one input layer, one output layer and one or more hidden layers (see Fig. 3).

The hidden layers of a Deep Neural Network could be fully connected (FC, a.k.a. dense layer), recurrent neural network (RNN) or convolutional neural network (CNN). In a FC, all neurons received as input all the weighted outputs of the preceding layer. Generally, it is followed by a non-linear activation function. In an RNN one neuron receives the preceding output of the previous layers and its own output of the previous values.

In particular, one of the most used layers in an RNN is the Long Short-Term Memory (LSTM). In LSTM the previous values are remembered over an arbitrary period of time, which makes these layers suitable for time series where the lags between events are uncertain. Moreover, the commonly input of an LSTM is a triplet consisting in: (samples, timesteps, features). The first value is the number of observations, the second value is the timesteps defined in (Equation 1), and the third value of the triplet is the number of features.

$$\frac{\text{windows size (in seconds)}}{\text{sampling rate (in seconds)}} \quad (1)$$

In a CNN, the outputs are convoluted, and one neuron only takes a subset of output signals (the closest outputs) of the previous layers (depending on the convolution of said outputs). CNN layers detect better the spatial component of the data — selecting the best features for us — and RNN detect better the temporal component of the data [11].

D. Signal Processing

We Bluetooth paired Muse headband to a mobile phone, through Mind-monitor App in order to collect EEG signals, raw data and brain waves derived from that. The raw EEG data consist in 4 signals coming from the 4 channels TP9, AF7, AF8, TP10 (See Fig. 4). The brain waves are derived from the raw EEG signals per each channel, consisting in the following wave

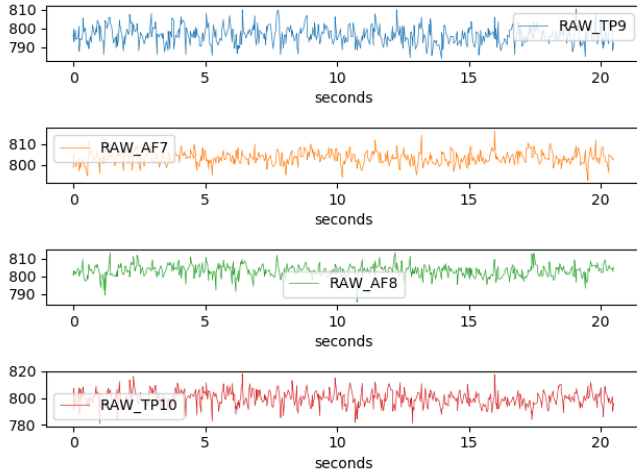


Fig. 4. Sample of raw EEG signal data through the four Muse channels

types: alpha, beta, theta, delta and gamma waves. A user's recording sample is shown in Fig. 5 for left- and right-hand motor imagery through these four channels, split by each type of wave. We found that raw EEG data do not report good results, and for that reason we only considered the brain waves data.

Therefore, we have a total amount of 20 brain wave signals (called features). All of these signals were recorded at the default sampling rate of 250Hz using 50% overlap between consecutive windows, and tested with several windows sizes (0.1s, 0.25s, 0.5s, 1s, 1.5s, 2s, 2.5s, 3s, 3.5s, 4s, 4.5s and 5s) in order to get the best performance (as in our previous work [20]). We did not choose a window size higher than 5 seconds in order to get an accurate model close to a real time performance. In this way, the lower window size, the better. Thus, we have different number of timesteps and samples depending on the different window sizes tested.

Table 1 shows the triplet corresponding to the different window sizes configurations (number of samples, timesteps and features) for the model input and samples in order to test the model performance. It is common to split the sample size in three datasets: 1) training dataset to build the model; 2) validation dataset is the unseen data by the training phase, used to tune parameters in the model; 3) and testing dataset is the new unused data in the training for validating the final model. In our case we use 3 users for training and validating and one user for testing. For the training and validation, it is common to split the datasets into 80%-20% and 90%-10% partitions depending on the available dataset size. In our case, for each of the 3 participant chosen for training and validating, we split the total number of samples of each participant into 90%-10%, (90% for training and 10% for testing), due to the small size of our dataset

TABLE I. MODEL INPUT CONFIGURATIONS FOR EVERY WINDOW SIZE

Window size	Model Input Triplet	Test samples
0.1s	(46687, 25, 20)	11672
0.25s	(17964, 62, 20)	4492
0.5s	(8876, 125, 20)	2220

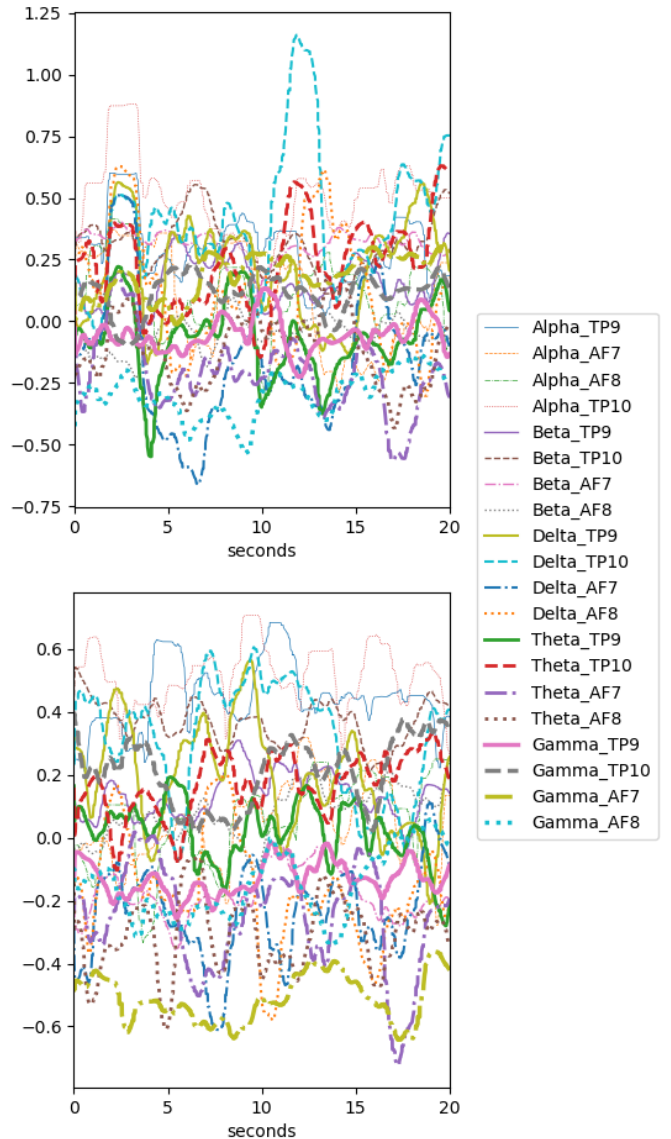


Fig. 5. Sample of a user's EEG signal for the five waves by channel

(Top) Brain waves for Left-hand motor imagery. (Bottom) Right-hand.

Window size	Model Input Triplet	Test samples
1s	(4324, 250, 20)	1081
1.5s	(2810, 375, 20)	703
2s	(2068, 500, 20)	518
2.5s	(1620, 625, 20)	405
3s	(1315, 750, 20)	329
3.5s	(1099, 875, 20)	275
4s	(947, 1000, 20)	237
4.5s	(800, 1125, 20)	200
5s	(717, 1250, 20)	180

E. Architecture Proposal

In this work, we propose a deep learning architecture based on CNN and LSTM layers (Fig. 6). CNN layer is used to extract the most relevant features (out of the initial 20) from the 5 brain waves and LSTM is used to classify the time series. Also, we tune the parameters of the layers (e.g. neurons) until we get the best performance, trying to reduce the values at the minimum in order to have a low computational model in terms of computational cost. The detailed description of architecture is the following:

- **The input layer.** This layer is three-dimensional following this triplet (samples: None, timesteps: 750, features: 20), explained in the previous subsection “Signal Processing”. These 750 timesteps correspond to the 3 seconds window size that reported the best performance presented in the Results section.
- **A CNN layer** with 32 filters of size 1.
- **A LSTM layer** with 32 neurons with 0.2 dropout and 0.001 regularizer, in order to prevent overfitting [21].

The implementation of the signal processing and the deep learning model architecture were coded with Python and Keras library [22]. In Keras, the samples value of the triplet is commonly set as “None” in the model architecture, because we do not know a priori the total amount of samples to use in the training phase. It means that the algorithm will accept any number of samples. Afterwards, when we train the model, we specify the samples split for training and validation.

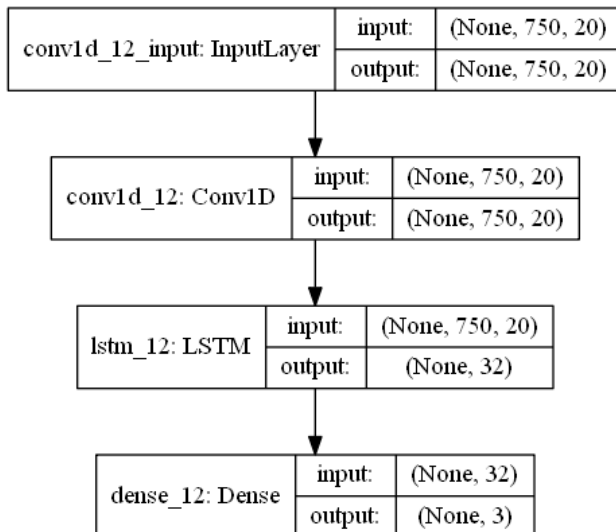


Fig. 6. Model Architecture Proposal with 3s window size

IV. RESULTS

We tested the deep learning architecture proposed with the different window size configurations. Table 2 presents the results obtained for all of them. The metrics used to evaluate the model were accuracy (Equation 2) and loss. Loss value in Keras is like the Mean Squared Error (MSE). Thus, the lower the loss value, the closer our predictions are to the true labels.

$$\frac{\text{Correct predictions}}{\text{Total predictions}} \quad (2)$$

The best configuration was achieved with 3 seconds window size, 98.9% accuracy and 0.05 loss in the training phase, while 96.5% accuracy and 0.25 loss in the validation phase. Furthermore, in the testing phase, the model reported 87% accuracy. Fig. 7 and Fig. 8 show the evolution of the accuracy and loss respectively through 300 epochs. And both of them indicate that our model is not overfitted, because the validation group follows the trend of the training accuracy and loss.

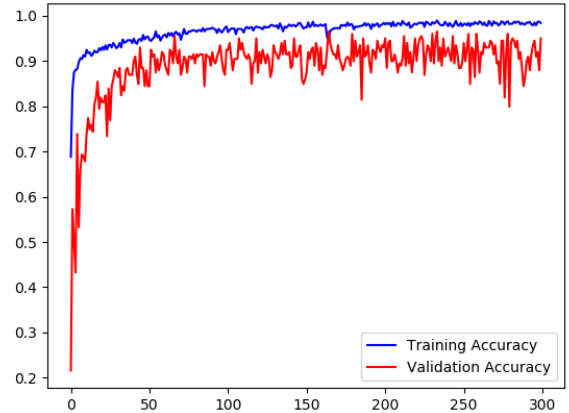


Fig. 7. Evolution of training and validation accuracies over 300 epochs

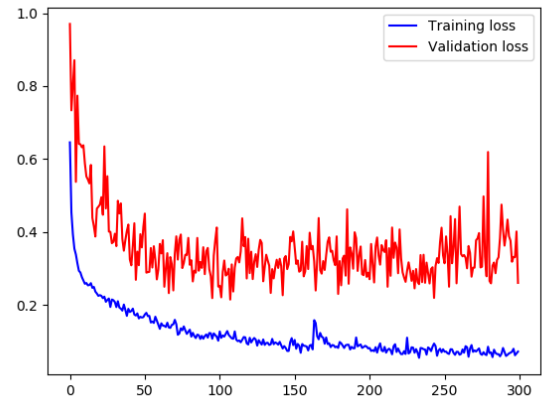


Fig. 8. Evolution of training and validation losses over 300 epochs

These results greatly improve the accuracy of similar previous works such as the experiments performed by Rodriguez et al. [16], which reaches an 80% accuracy, and Li et al. [17] with a 95.1% accuracy. Our proposal overcomes the accuracy of [16] by 16.5%, and it is 1.4% higher than [17]. We also take recordings of a higher number of users than they take (3 versus one), and we recruited another user for testing our model. We used five types of waves per channel (20 features) instead of raw data used in [16] or the gamma waves of AF7 and AF8 channels used in [17]. We also avoided model overfitting

using dropout layers and regularizers. Moreover, we tested different window sizes to find the best configuration, and we validated the model in each epoch.

TABLE II. MODEL PERFORMANCE FOR DIFFERENT WINDOW SIZE CONFIGURATIONS

W size	Train Loss	Train Acc	Val Loss	Val Acc	Test Acc
0.1s	0.052848	0.987276	0.675215	0.866933	0.891575
0.25s	0.055006	0.984421	0.485793	0.878383	0.860330
0.5s	0.044987	0.987422	0.490147	0.892804	0.697148
1s	0.05377	0.986971	0.368562	0.927803	0.769159
1.5s	0.057503	0.984538	0.312799	0.926714	0.895265
2s	0.055652	0.985860	0.309958	0.929487	0.733202
2.5s	0.060357	0.984881	0.334550	0.930894	0.756410
3s	0.054438	0.989343	0.256634	0.964824	0.868339
3.5s	0.05078	0.990426	0.422187	0.886228	0.816479
4s	0.058723	0.987715	0.357903	0.923611	0.818584
4.5s	0.050014	0.994152	0.502173	0.851240	0.912821
5s	0.068768	0.987118	0.391484	0.890909	0.771084

W: Window. Acc: Accuracy. Val: Validation.

We confirmed the influence of the brain waves captured by the channels AF7 and AF8 [17], while a user is imagining its hand moving to pick a bottle up with his eyeballs rotated in the same direction. As can be seen in Fig. 9 and Fig. 10 we can detect some activity in these waves. Fig. 9 presents the gamma signal through AF7 and AF8 of a user. In this case only with these signals we could detect the user motor imagery. However, Fig. 10 shows that this situation is not generalized in all cases. In Fig. 10 another user has gamma activity, but it is not straightforward to detect which hand the user is thinking to move only with these signals. To evaluate this assertion, we train and validate our deep learning architecture only with these 2 features (gamma AF7 and gamma AF8) instead of the 20 selected, and the accuracy was very low, close to 2%. Although Li et al. [17] use only the gamma waves for their one user study, we demonstrated that this behavior could not be generalized, and we need to include in our study the 5 types of waves and use deep learning to detect the motor imagery.

Additionally, the four users reported a good usability of the system during the experiment. They felt very good wearing the headband because it is comfortable, data were collected in a transparent way for them, and it is low-invasive.

V. CONCLUSIONS

In this work, the results showed that motor imagery classification, with low-cost and low-invasive headband, for left and right hands is feasible and accurate. The proposed deep learning model architecture, based on a CNN layer and a LSTM layer, ensure a validation accuracy of 96.5%. Moreover, we found that the 5 types of waves (alpha, beta, theta, delta and gamma) through TP9, TP10, AF7 and AF8 channels are needed

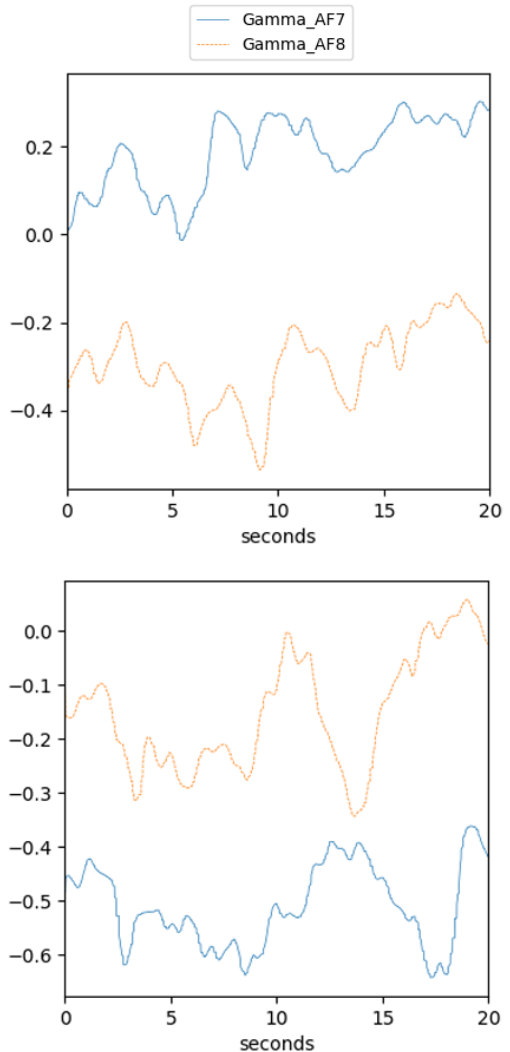


Fig. 9. User sample EEG signal for gamma wave and channels AF7 and AF8
(Top) Brain waves for Left-hand motor imagery. (Bottom) Right-hand.

for an accurate classification. Besides, we have observed that the raw data is not enough to ensure the accuracy of the results.

This proposal has the potential of increasing people independence, allowing them to interact with computer systems and applications without using their bodies, but just thinking or imagining the movement.

Our proposal has some limitation. Although Muse headband is low-invasive compared to similar BCI devices, it is still intrusive and awkward to wear in outdoors activities. In the future probably other non-intrusive devices will appear which will make them suitable for outdoors activities. Another limitation is the size of our sample.

For the future work, we will increase the sample size, and we will integrate our model with our previous e-health system and extend the detection to other types of motor imagery. We will also explore the possibility of predicting motor imagery in real-

time. This is not an irrelevant task, as in real life we have to offer an immediate response, and 3 seconds windows, which reported as the best accuracy in our experiments, could slow down the user experience. In addition, we will increase the sample size in order to build a better accurate model able to generalize, which could reach a higher percentage of accuracy than the presented here, not only in the training and validation, but also in testing. Furthermore, the properties of Muse headband such as low-cost and low-invasive contribute to democratize the adoption of these BCI wearable technologies in the health domain. In this line, other of our objectives is the recognition of activities, mental state and emotions of the users while they are performing daily life activities and the relationship with their health status. The headband will be part of our system based on microservices and cloud, which includes other wearable sensors and applications to monitor and intervene in the healthcare of the elderly. Thus, the integration of the proposal presented in this paper with our previously designed e-health system will be able to contribute to a practical solution for the healthcare systems.

ACKNOWLEDGMENT

This research work is funded by the Spanish Ministry of Economy and Competitiveness - Agencia Estatal de Investigación - with European Regional Development Funds (AEI/FEDER, UE) through the project reference TIN2016-79484-R, and the FPU scholarship FPU18/00287 granted by the Spanish Ministry of Education and Professional Training.

APPENDIX A. LIST OF ACRONYM

ADLs	Activities of daily living
AFX	Position of an electrode in BCI, with number X
API	Application Programming Interface
BCI	Brain Computer Interfaces
CNN	Convolutional Neural Network
DL	Deep Learning
EEG	Electroencephalography
Fpz	Reference electrode in BCI
LSTM	Long Short-Term Memory
MSE	Mean Squared error
NN	Neural Network
RNN	Recurrent Neural Network
SDK	Software Development Kits
SVM	Support Vector Machines
TPX	Position of an electrode in BCI, with number X

REFERENCES

- [1] J. Dunn, R. Runge, and M. Snyder, "Wearables and the medical revolution," *Per. Med.*, vol. 15, no. 5, pp. 429–448, Sep. 2018.
- [2] S. Enshaeifar et al., "Health management and pattern analysis of daily living activities of people with dementia using in-home sensors and machine learning techniques," *PLoS One*, vol. 13, no. 5, p. e0195605, May 2018.
- [3] G. Fico et al., "Co-creating with consumers and stakeholders to understand the benefit of Internet of Things in Smart Living Environments for Ageing Well: the approach adopted in the Madrid Deployment Site of the ACTIVAGE Large Scale Pilot," in *IFMBE Proceedings*, vol. 65, 2018, pp. 1089–1092.
- [4] García-Moreno et al., "Designing a Smart Mobile Health System for

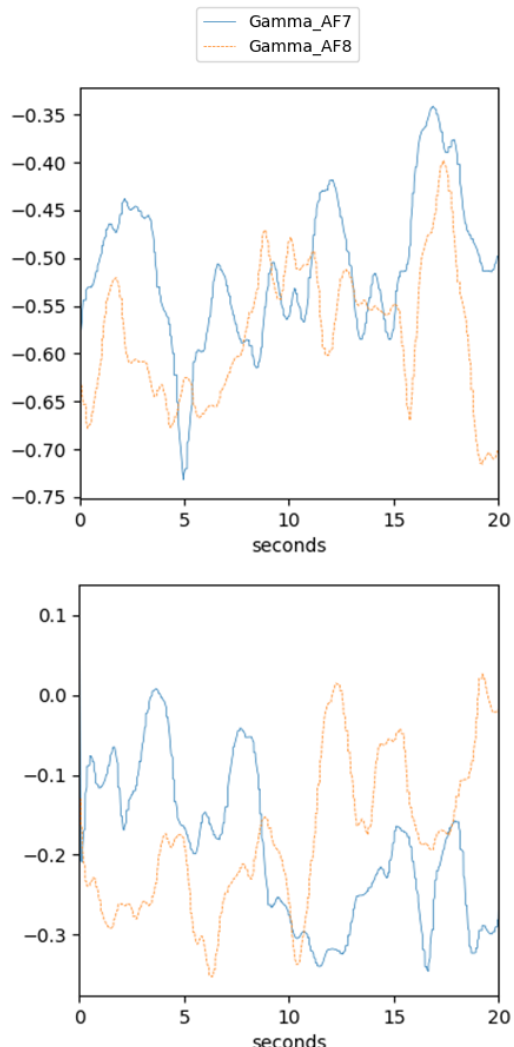


Fig. 10. Another user sample EEG signal for gamma wave and channels AF7 and AF8

(Top) Brain waves for Left-hand motor imagery. (Bottom) Right-hand.

Ecological Frailty Assessment in Elderly," *Proceedings*, vol. 31, no. 1, p. 41, Nov. 2019.

- [5] Interaxon, "Muse 2: Brain Sensing Headband - Technology Enhanced Meditation." [Online]. Available: <https://choosemuse.com/muse-2/>. [Accessed: 27-Jan-2020].
- [6] V. Jurcak, D. Tsuzuki, and I. Dan, "10/20, 10/10, and 10/5 systems revisited: Their validity as relative head-surface-based positioning systems," *Neuroimage*, vol. 34, no. 4, pp. 1600–1611, Feb. 2007.
- [7] M. Bermudez-Edo and P. Barnaghi, "Spatio-Temporal Analysis for Smart City Data," in *Companion of the The Web Conference 2018 on The Web Conference 2018 - WWW '18*, 2018, pp. 1841–1845.
- [8] Y. LeCun, Y. Bengio, and G. Hinton, "Deep learning," *Nature*, vol. 521, no. 7553, pp. 436–444, May 2015.
- [9] J. Ngiam, A. Khosla, M. Kim, J. Nam, H. Lee, and A. Y. Ng, "Multimodal

- Deep Learning,” 2011.
- [10] D. Ravi et al., “Deep Learning for Health Informatics,” *IEEE J. Biomed. Heal. Informatics*, vol. 21, no. 1, pp. 4–21, Jan. 2017.
- [11] Y. Roy, H. Banville, I. Albuquerque, A. Gramfort, T. H. Falk, and J. Faubert, “Deep learning-based electroencephalography analysis: a systematic review,” *J. Neural Eng.*, vol. 16, no. 5, p. 051001, Aug. 2019.
- [12] J. J. Bird, D. R. Faria, L. J. Manso, A. Ekárt, and C. D. Buckingham, “A Deep Evolutionary Approach to Bioinspired Classifier Optimisation for Brain-Machine Interaction,” *Complexity*, vol. 2019, pp. 1–14, Mar. 2019.
- [13] G. Wiechert et al., “Identifying users and activities with cognitive signal processing from a wearable headband,” in *2016 IEEE 15th International Conference on Cognitive Informatics & Cognitive Computing (ICCI*CC)*, 2016, pp. 129–136.
- [14] J. Zhang, Z. Jadavji, E. Zewdie, and A. Kirton, “Evaluating If Children Can Use Simple Brain Computer Interfaces,” *Front. Hum. Neurosci.*, vol. 13, no. February, pp. 1–7, Feb. 2019.
- [15] W. Chen et al., “EEG-based Motion Intention Recognition via Multi-task RNNs,” in *Proceedings of the 2018 SIAM International Conference on Data Mining*, Philadelphia, PA: Society for Industrial and Applied Mathematics, 2018, pp. 279–287.
- [16] P. I. Rodriguez, J. Mejia, B. Mederos, N. E. Moreno, and V. M. Mendoza, “Acquisition, analysis and classification of EEG signals for control design.”
- [17] Z. Li, J. Xu, and T. Zhu, “Recognition of Brain Waves of Left and Right Hand Movement Imagery with Portable Electroencephalographs,” Sep. 2015.
- [18] J. Clutterbuck, “Mind Monitor.” [Online]. Available: <https://mind-monitor.com/>. [Accessed: 27-Jan-2020].
- [19] B. K. Bodenseo, “Machine Learning with Python: Neural Network with Python using Numpy.” [Online]. Available: https://www.python-course.eu/neural_networks_with_python_numpy.php. [Accessed: 02-Feb-2020].
- [20] M. Bermudez-Edo, P. Barnaghi, and K. Moessner, “Analysing real world data streams with spatio-temporal correlations: Entropy vs. Pearson correlation,” *Autom. Constr.*, vol. 88, pp. 87–100, Apr. 2018.
- [21] G. Pereyra, G. Tucker, J. Chorowski, L. Kaiser, and G. Hinton, “Regularizing Neural Networks by Penalizing Confident Output Distributions,” *ICLR Work.*, Jan. 2017.
- [22] F. Chollet and others, “Keras,” 2015. [Online]. Available: <https://keras.io>.